

Article

Utilization of Waste Brick Powder as a Partial Replacement of Portland Cement in Mortars

Zhuomin Zou , Samuel Provoost and Elke Gruyaert * 

Department of Civil Engineering, Faculty of Engineering Technology, Materials and Constructions,
Ghent Campus, KU Leuven, 9000 Ghent, Belgium

* Correspondence: elke.gruyaert@kuleuven.be; Tel.: +32-9-331-65-97

Abstract: Partially substituting Portland cement (PC) with waste brick powder (WBP) is an effective method to reduce environmental pollution. In this paper, the effects of a WBP with low pozzolanic activity on the fresh and hardened properties of blended cement with 0–40% WBP or 50% of WBP+GGBFS (by mass) were studied. Sodium sulphate (SS) (1.5 and 2.5%, related to powder mass) was used to activate the blended cement with 40% WBP or 50% WBP+GGBFS at 20 °C. Results show that the performance of blended cement is decreased with the increase in WBP content since the WBP with low pozzolanic activity mainly contributes to the dilution effect. Binary cement with 10% WBP shows a similar carbonation depth and chloride migration coefficient to PC. Ternary cement with 10% WBP and 40% GGBFS exhibits a slightly lower strength at 90 days and a lower chloride migration coefficient than PC. The SS solution increases the compressive strength at 2 days and decreases the compressive strength at 28 and 90 days. Moreover, the SS solution results in a lower carbonation depth and chloride migration coefficient, except for ternary cement with 10% WBP and 40% GGBFS, which shows a higher carbonation depth at 42 and 68 days. This paper provides a reference for the application of WBP to produce green mortars.

Keywords: waste brick powder; ground granulated blast-furnace slag; sodium sulphate; blended cement



Citation: Zou, Z.; Provoost, S.; Gruyaert, E. Utilization of Waste Brick Powder as a Partial Replacement of Portland Cement in Mortars. *Sustainability* **2024**, *16*, 624. <https://doi.org/10.3390/su16020624>

Academic Editor: Christopher Cheeseman

Received: 2 November 2023

Revised: 6 January 2024

Accepted: 8 January 2024

Published: 11 January 2024



Copyright: © 2024 by the authors. Licensee MDPI, Basel, Switzerland. This article is an open access article distributed under the terms and conditions of the Creative Commons Attribution (CC BY) license (<https://creativecommons.org/licenses/by/4.0/>).

1. Introduction

Since Portland cement (PC) production accounts for a large share of anthropogenic CO₂ emissions, using supplementary cementitious materials (SCMs), such as ground granulated blast-furnace slag (GGBFS), fly ash and limestone, to partially replace Portland clinker is a common way to reduce the environmental impact. The European Standards EN 197-1 [1] and EN 197-5 [2] list 32 common cements with main components other than Portland clinker in contents varying between 11% and 95%. However, the availability of these SCMs is facing challenges. The supply of fly ash has been reduced with the closure of coal-fired power plants, and GGBFS production is dependent on local pig iron production [3]. Hence, it is necessary to extend the variety of SCMs.

In Europe, 200 million tonnes of construction and demolition waste are generated every year, of which ceramics and bricks account for approximately 30–40% [4,5]. During burning in brick production, the crystalline structure of the raw materials, clay minerals, is dehydroxylated to form a reactive amorphous structure, leading to pozzolanic activity [6]. From [7], the optimal kaolin burning temperature is around 700 °C, as crystallization occurs at temperatures over 900 °C and less amorphous products are formed at temperatures below 700 °C. After grinding the waste brick into powders with a suitable particle size distribution (PSD) with a D₉₀ value normally lower than 150 μm (D₉₀ corresponds to the particle size at which the cumulative particle size distribution reaches 90%), the WBP can be used to partially replace PC in mortars or concretes [6,8–12]. Previous studies have suggested that mortars or concretes with PC replaced by 20–30% WBP could exhibit similar fresh and hardened properties to reference mortars or concretes without WBP [8,10,12].

On the one hand, WBP particles finer than PC can fill the voids between the PC particles and increase the packing density of the mixture. On the other hand, calcium aluminate hydrates (C-A-H) and calcium aluminium silicate hydrates (C-A-S-H) are generated from the reaction between WBP and the PC hydration product $\text{Ca}(\text{OH})_2$, resulting in a dense microstructure [10–12]. Hence, the pozzolanic activity of WBP has a significant effect on the performance of blended cement.

To improve the pozzolanic reactivity of WBP, mechanical grinding and alkali activation have been widely applied [13–15]. In [15], the Si-O and Al-O bond energies of the WBP are decreased as the D50 value (D50 corresponds to the particle size at which the cumulative particle size distribution reaches 50%) decreases from 27.1 μm to 3.4 μm , indicating an improvement in the pozzolanic activity. Moreover, the compressive strength of blended cement containing 30% WBP with a D50 of 3.4 μm is approximately 10% lower than that of PC with a D50 of 13.5 μm . For the alkali-activated method, calcium silicate hydrates (C-S-H) and C-A-S-H gels are the main products in the case of high-calcium materials, while sodium aluminium silicate hydrate (N-A-S-H) gels are the main products in the case of low-calcium materials when activated by an alkaline solution such as Na_2SiO_3 and NaOH , resulting in good performance [16–19]. Several studies showed that the compressive strength of blended cement with WBP activated by Na_2SiO_3 and NaOH solution is higher than that without an alkaline activator [5,13,20–22]. However, the better mechanical performances of mortars with alkali-activated WBP are usually achieved by curing them at an elevated temperature ranging from 40 to 80 $^\circ\text{C}$ [5,13,20–22], which limits their application in the construction sector. Moreover, the high production cost and high corrosive behaviour of NaOH solid/solution makes its use on a large scale relatively impractical [23]. Sodium sulphate (Na_2SO_4 , SS), with a low alkalinity obtained from sulphate-bearing brines and a hydrochloric acid manufacture process, has been used as an alternative activator that allows alkaline materials to be used in the construction industry [24]. SS can react with $\text{Ca}(\text{OH})_2$ from the hydration of PC to generate NaOH , which improves the alkalinity in the pore solution [25]. From [26], it seems that blended cement with 50% fly ash (particle size below 45 μm) activated by 5% (related to the mass of fly ash) SS solution exhibits an ~8% lower compressive strength than the PC without SS at 7 and 28 days. In [27], the compressive strength of mortars with 100% ultra-fine slag (D50 = 3.1 μm) activated by 4% (Na_2O equivalent of the blends) SS solution reached 36.2 MPa and 77.3 MPa at 28 and 90 days, respectively.

Previous studies suggest that the replacement of 20–30% of PC by WBP without alkaline activators can be applied with insignificant harm to technological properties [6,15]. Hence, the purpose of this work was to assess the effects of higher replacement ratios of PC by WBP (up to 40% by mass) on typical fresh and hardened properties of mortars. Moreover, to replace 50% PC, combinations of WBP with a more reactive supplementary cementitious material, here GGBFS, were made. Since the pozzolanic activity of the WBP used in the current study was quite low, it was investigated whether 1.5 and 2.5% SS (related to powder mass) were useful to activate blended cement with 40% WBP or 50% of WBP+GGBFS at room temperature (20 $^\circ\text{C}$). The fresh and hardened properties of the mortars were studied in terms of flow table value, flexural strength, compressive strength, carbonation and non-steady-state chloride migration.

2. Materials and Methods

2.1. Materials

Commercial PC (CEM I 42.5 N) from Heidelberg and GGBFS from ECOCEM were used to blend the WBP to prepare mortars. The WBP came from a brickyard where high-speed building bricks are perfectly ground to size for gluing. The PSD curves of the powders were measured using a laser diffraction particle size analyser (Fritsch type analysette 22), as shown in Figure 1. Table 1 shows the comparison of the particle size distribution of PC, GGBFS and WBP based on the D10, D50 and D90 values. The PC and GGBFS show a similar particle size distribution, while the WBP has a slightly coarser particle size distribution

with higher D50 and D90 values. The chemical compositions of the powders measured using X-ray fluorescence (XRF) are shown in Table 2 and the mineralogical phases of the WBP measured using X-ray diffraction (XRD) are shown in Table 3. The PC has the highest CaO content and lowest SiO₂ content, while the WBP shows the lowest CaO content and highest SiO₂ content. Compared with PC, the GGBFS is richer in SiO₂, Al₂O₃ and MgO. The mineralogical phases of the WBP indicate that the amorphous content of the WBP is quite low. The sand used in mortars was river sand with a size range of 0–4 mm. Anhydrous SS powder was used as the alkaline activator with a density of 2.7 g/cm³ (20 °C).

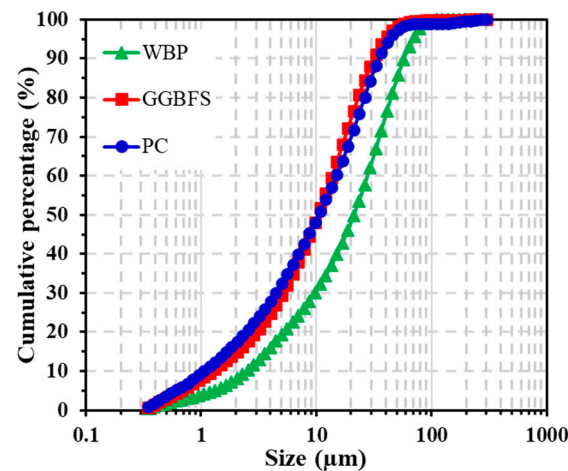


Figure 1. Particle size distribution of binder materials.

Table 1. The D10, D50 and D90 of the particle size distribution of PC, GGBFS and WBP.

	D10 (μm)	D50 (μm)	D90 (μm)
PC	1.1	10.4	35.0
GGBFS	1.2	10.3	31.6
WBP	2.7	21.1	57.2

Table 2. The chemical compositions of PC, GGBFS and WBP determined via XRF analyses.

	Chemical Composition (wt.%)													
	CaO	SiO ₂	Al ₂ O ₃	Fe ₂ O ₃	K ₂ O	MgO	Mn ₂ O ₃	Na ₂ O	Cr ₂ O ₃	TiO ₂	SO ₃	P ₂ O ₅	Cl ⁻	S ²⁻
PC	65.5	18.1	4.4	3.64	0.72	1.81	-	0.25	-	0.48	4.29	0.35	-	-
GGBFS	41.1	34.3	10.2	0.6	0.47	6.8	-	0.93	-	0.7	0.1	-	0.02	0.7
WBP	9.51	71.13	10.14	3.82	2.25	1.31	0.06	0.68	0.03	1.09	-	-	-	-

Table 3. The mineralogical phases of the WBP determined via XRD analyses.

	Mineralogical Phases and Amorphous Content (wt.%)						
	Quartz	Albite	Alkali Feldspar	Melilite Group	Clinopyroxene	Hematite	Amorphous
WBP	38.3	14.9	9.1	2.3	8.5	2.1	24.7

The mix proportions of the mortars are provided in Table 4. Experiments were carried out on mortars with a water-to-binder ratio of 0.5 and a sand-to-binder ratio of 3.0. SS (1.5 and 2.5%) was used to activate binary cement with 40% WBP and ternary cements with 50% of WBP+GGBFS. The SS solution was prepared with a mix of water and SS powder 24 h before making mortars. The pure PC (C100) and binary cement with 50% GGBFS (C50S50) were selected as reference mixtures. The mortars were prepared according to NBN EN

196-1 [28]. Fresh mortar was cast into moulds (40 × 40 × 160 mm) with a plastic cover and cured in a lab environment for 24 h. Then, the mortar samples were demoulded and cured in a water tank at 20 °C until the test age.

Table 4. Mix proportion of specimens.

Series	Code	Na ₂ SO ₄ (g)	Binder (g)			Water (g)	Sand (g)
			PC (g)	WBP (g)	GGBFS (g)		
Reference	C100	-	450	-	-	225	1350
	C50S50	-	225	-	225	225	1350
	C90B10	-	405	45	-	225	1350
	C75B25	-	337.5	112.5	-	225	1350
	C60B40	-	270	180	-	225	1350
	C50B10S40	-	225	45	180	225	1350
	C50B25S25	-	225	112.5	112.5	225	1350
	C50B40S10	-	225	180	45	225	1350
	1.5% SS	C60B40	6.75	270	180	-	225
C50B10S40		6.75	225	45	180	225	1350
C50B25S25		6.75	225	112.5	112.5	225	1350
C50B40S10		6.75	225	180	45	225	1350
2.5% SS	C60B40	11.25	270	180	-	225	1350
	C50B10S40	11.25	225	45	180	225	1350
	C50B25S25	11.25	225	112.5	112.5	225	1350
	C50B40S10	11.25	225	180	45	225	1350

2.2. Test Methods

The pozzolanic activity of WBP was measured using the Frattini test according to NBN EN 196-5 [29]. Three independent tests were conducted for each mix proportion. In the Frattini test, 100 mL of freshly boiled water was firstly sealed into a polyethylene container at 40 °C for at least 1 h to reach a uniform temperature. Then, 20 g of blended cement was added into the container and shaken for 20 s to avoid cement lumps. The polyethylene container was stored at 40 °C until the test ages (7 and 28 days). Then, samples were filtered into a vacuum flask and 50 mL solution was pipetted into a 250 mL beaker. The hydroxyl ion concentration, [OH]⁻, was determined with 0.1 mol/L HCl and five drops of methyl orange were used as the indicator. The titration end-point corresponded to the colour changing from yellow to orange. The [OH]⁻ can be calculated following Equation (1):

$$[OH]^{-} = 2 \times V_1 \times f_1 \quad (1)$$

where V_1 (mL) is the volume of 0.1 mol/L HCl solution used for the titration and f_1 is the factor of 0.1 mol/L HCl solution, which was determined as follows: (0.200 ± 0.001) g sodium carbonate was mixed with 75 mL water into a flask. Then, the solution was titrated with 0.1 mol/L HCl and five drops of methyl orange were used as the indicator. The titration end-point corresponded to the colour changing from yellow to orange.

Then, the titrated solution was adjusted to a pH of 12.5 ± 0.2 with 2.5 N NaOH solution. After that, around 0.1 g Patton and Reeders reagent indicator was added in the solution and 0.03 mol/L EDTA solution was used for titration until the colour changed from purple to clear blue. The calcium oxide (CaO) concentration is calculated according to Equation (2):

$$CaO = 0.6 \times V_2 \times f_2 \quad (2)$$

where V_2 (mL) is the volume of EDTA solution used for the titration and f_2 is the factor of the EDTA solution, which can be determined by use of calcium carbonate. An amount of (1.00 ± 0.01) g calcium carbonate was mixed with 100 mL water into a beaker. Approximately 10 mL of 4 mol/L HCl was added in the beaker to dissolve the calcium carbonate.

The solution was boiled to expel the dissolved CO₂ and then cooled to room temperature. The solution was transferred into a volumetric flask and mixed with water up to 1000 mL. Then, 50 mL solution was pipetted to adjust its pH to 12.5 ± 0.2 by 2.5 N NaOH. After that, around 0.1 g Patton and Reeders reagent indicator was added to the solution and 0.03 mol/L EDTA solution was used for titration until the colour changed from purple to clear blue.

The flow table test of mortars was measured according to NBN EN 1015-3 [30]. The conical mould placed on the disc of the flow table was filled with mortar in two layers. Each mortar layer was compressed by 10 strokes of the tamper to ensure a uniform distribution. After the removal of the mould, mortars were spread on the disc by jolting the flow table 15 times. The flow value was the mean value of the diameters in two directions at right angles. Three independent tests were conducted for each mix proportion.

Strength tests on mortars were executed at 2, 7, 28 and 90 days according to NBN EN 196-1 [28]. For the flexural strength test, three specimens with dimensions of $40 \times 40 \times 160$ mm were broken into six pieces via three-point bending tests at a loading rate of 50 ± 10 N/s. The compressive strength was evaluated on the six broken pieces at a loading rate of 2400 ± 200 N/s on a cross-sectional area of 40×40 mm.

The carbonation test was conducted based on NBN EN 13295 [31]. After demoulding, three mortar specimens were cured in a water tank for 28 days. Subsequently, specimens were stored in a climate chamber ($T = 20 \pm 2$ °C, $RH = 60 \pm 10\%$) for another 14 days. Before the start of the carbonation test, the initial carbonation depth of the specimens was measured and was equal to zero. Then, specimens were placed in the carbonation chamber ($T = 20 \pm 2$ °C, $RH = 60 \pm 10\%$ and 1 vol% CO₂ level) for 14, 42 and 68 days. The carbonation depth was determined by spraying phenolphthalein solution on a freshly split surface and was measured at five points on each side to the nearest 0.1 mm.

The non-steady chloride migration test was performed in accordance with NT BUILD 492 [32]. Three cylindrical mortar specimens with a diameter of 100 mm and a height of 200 mm were prepared. After curing in a water tank for 28 or 56 days, thick slices of 50 ± 2 mm were obtained by cutting the cylindrical specimens. Then, the thick slices (3 per mix and per test age) were placed in a vacuum container for three hours. With the vacuum pump still running, the container was filled with saturated Ca(OH)₂ solution until all slices were immersed. The vacuum condition was maintained for another hour and slices were kept in the solution for 18 ± 2 h. A 0.3 N NaOH and a 2 N NaCl solution were used as anolyte and catholyte solutions, respectively. The end surface that was near to the middle surface of the original mortar cylinder was the one to be exposed to the chloride solution (catholyte).

An analysis of variance (ANOVA) was conducted by use of SPSS version 26.0 for Windows (SPSS Inc., Chicago, IL, USA). A value of $p < 0.05$ was considered significant. Statistical analysis was conducted on at least three independent measurements per series according to the flowchart in Figure 2a. Figure 2b exemplifies the method of working with the case in which the compressive strength results at 90 days for C100, C90B10 and C25B75 were analysed. The Shapiro–Wilk test showed that the significance level was larger than 0.05, indicating a normal distribution of the data. Then, the homogeneity of variances was tested based on Levene’s test and the significance level was lower than 0.05, indicating unequal variances. Finally, the ANOVA with Dunnett T3 post hoc test was used for multi-comparison of the data and the significance level was lower than 0.05, indicating a significant difference among the compressive strengths of C100, C90B10 and C25B75 at 90 days.

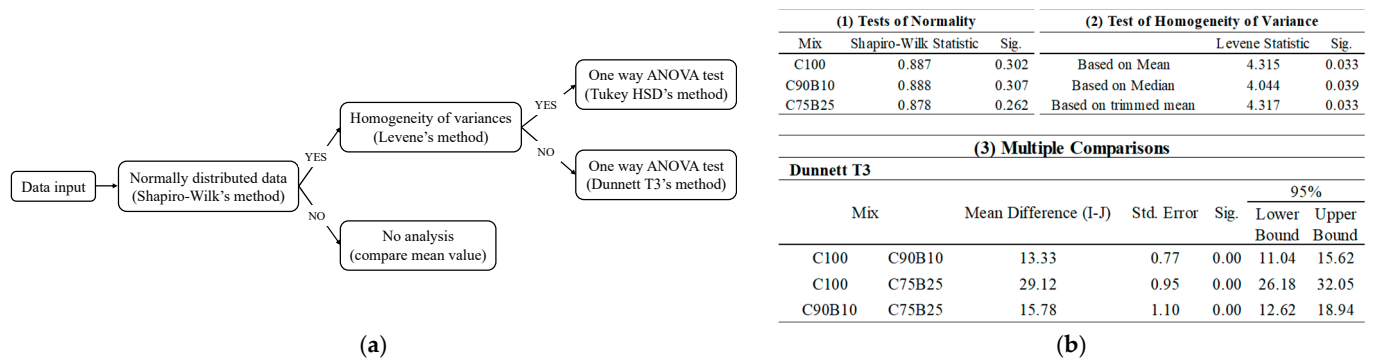


Figure 2. The statistical methodology used in this paper: (a) flowchart of the statistical analysis; (b) an example of the outcomes of the statistical test comparing compressive strength results at 90 days among C100, C90B10 and C25B75.

3. Results and Discussion

3.1. Pozzolanic Acitivity

The amorphous content; the CaO, Al₂O₃ and SiO₂ content; and the D10, D50, D90 values of the WBP used in the current study are compared with those of other waste brick powders, being waste products from the grinding of bricks used for mortar-free masonry walling in [7] and from a demolition site in [6,15] (Table 5). Results in [7] indicate that the pozzolanic activity of brick powder is increased with the increase in amorphous content, and the decrease in PSD has a positive effect on the improvement in the pozzolanic activity. From [15], the particle shape of the brick powder tends to be spherical with the decrease in particle size from D50 = 27.1 μm (brick 7) to D50 = 3.4 μm (brick 10), which increases the contact area of materials and decreases the surface binding energy to improve its pozzolanic activity. Compared with brick powders 1–6, the WBP used in the current study has a lower amorphous content with lower CaO and Al₂O₃ contents and a higher SiO₂ content, indicating obviously lower pozzolanic activity. On the contrary, compared with the powders of bricks 7–10, the WBP used in the current study shows more CaO, less Al₂O₃ and more SiO₂, while it shows a similar amorphous content and quite similar PSD to brick powder 8, which has demonstrated that it can be used to replace PC by up to 20% in mortars. The results of the Frattini test for blended cement at 7 and 28 days are shown in Figure 3. The calcium isotherm curve divides the graph into pozzolanic and non-pozzolanic areas, respectively, below and above this curve. Figure 3a shows that the pozzolanic activity of blended cement with WBP is increased with WBP content and curing ages. The value of C90B10 at 7 days is above the solubility line corresponding to no pozzolanic activity. The results for C90B10 at 28 days and C75B25 at 7 days lie near, but below, the line, indicating a poor pozzolanic activity. The C60B40 shows high pozzolanic reactivity at both 7 and 28 days while C75B25 has a good value at 28 days. Figure 3b shows that all points of blended cement with GGBFS and WBP are below the isotherm curve except C50S50 at 7 days.

3.2. Flow Table

Figure 4 shows the flowability of mortars with and without SS. There is an insignificant difference in flow values between C100 and C50S50 ($p = 0.70$). The difference is significant between C100/C50S50 and binary cements with 10–40% WBP or ternary cement with 50% of WBP+GGBFS ($p < 0.05$). C100 and C50S50 show obviously higher flow values than the other binary and ternary cements (Figure 4a). Moreover, the mortars without SS solution, except C100 and C50S50, show an insignificant difference in flow value ($p > 0.05$). The mean flow value of the mortars is slightly decreased with the increase in WBP content for both binary cement with WBP and ternary cement with WBP and GGBFS.

Table 5. The amorphous content; CaO, Al₂O₃ and SiO₂ content; and D10, D50, D90 of the WBP used in this study and brick powders (bricks 1–6 from [7] and bricks 7–10 from [15]).

Materials	Pozzolanic Activity (mg Ca(OH) ₂ /1 g Pozzolan) after 1 Day	Amorphous (%)	CaO (%)	Al ₂ O ₃ (%)	SiO ₂ (%)	D10 (μm)	D50 (μm)	D90 (μm)
WBP	-	24.7	9.51	10.13	71.13	1.3	15.1	41.0
Brick 1	460	72.1	13.79	15.61	58.50	1.8	16.6	95.6
Brick 2	455	71.3	14.10	15.14	58.34	1.6	10.6	48.3
Brick 3	408	65.2	15.10	15.25	58.12	1.6	12.3	70.6
Brick 4	345	65.4	10.15	15.19	59.12	1.6	15.2	222.3
Brick 5	326	64.3	10.24	15.10	58.87	1.7	13.5	94.6
Brick 6	296	63.7	10.57	15.24	58.13	1.8	13.4	154.1
Brick 7	-	20.1	1.9	18.4	64.5	5.0	27.1	91.2
Brick 8	-	20.1	1.9	18.4	64.5	1.6	15.8	55.3
Brick 9	-	20.1	1.9	18.4	64.5	1.0	10.5	33.3
Brick 10	-	20.1	1.9	18.4	64.5	0.6	3.4	24.1

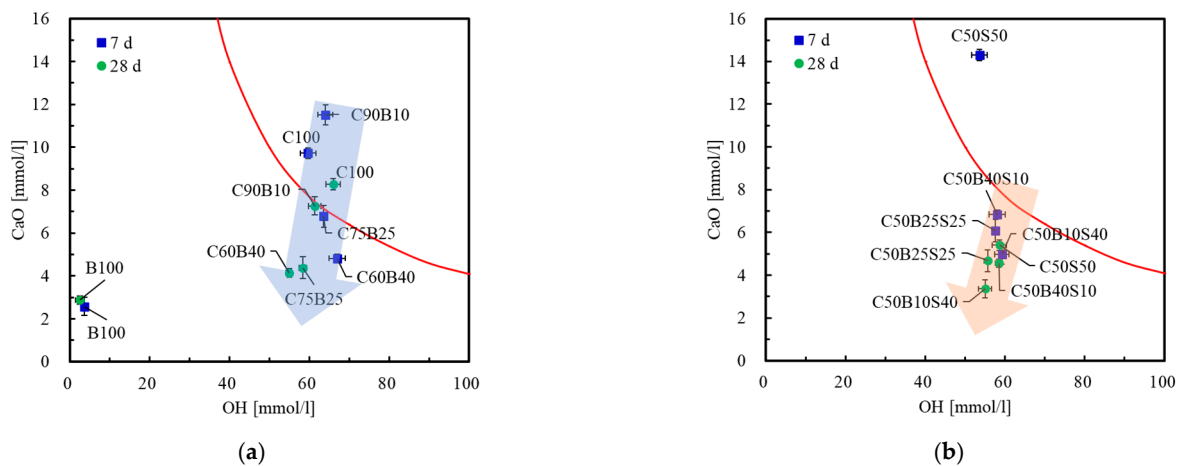


Figure 3. Frattini test results for blended cement at 7 and 28 days: (a) blended cement with WBP; (b) blended cement with GGBFS and WBP.

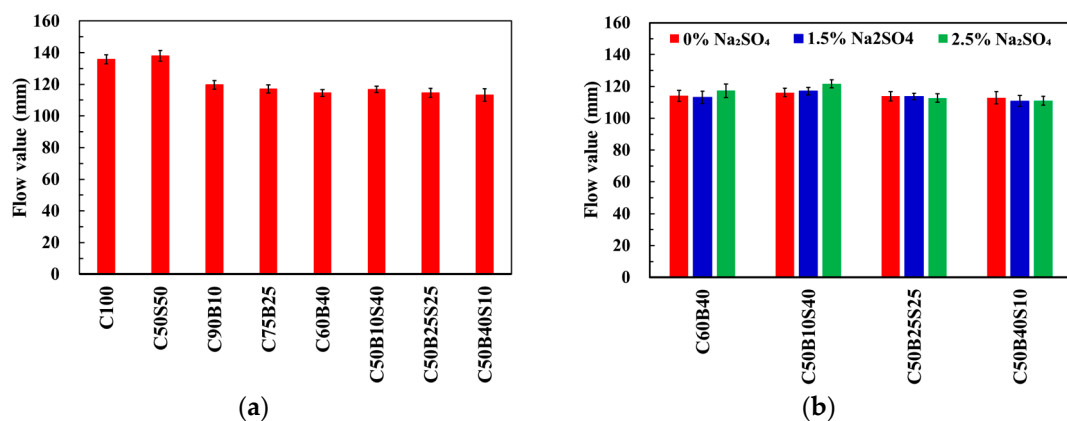


Figure 4. Flow values of mortars with and without SS: (a) mortars without SS; (b) mortars with 0%, 1.5% and 2.5% SS.

Figure 4b shows the comparison of flow values for mortars with different SS contents. There is an insignificant difference in the flow value between mortars with 0%, 1.5% and 2.5% SS solution ($p > 0.05$). The C60B40 and C50B10S40 activated by 2.5% SS have a slightly higher mean flow value than those activated by 0% and 1.5% SS. The mini-slump test

in [24] indicated that a content of SS ranging from 1% to 3% (Na_2O equivalent of Na_2SO_4 by the mass of slag) has little effect on the workability of SS-activated GGBFS pastes at a water-to-binder ratio of 0.3.

3.3. Flexural and Compressive Strength

The flexural strength results of mortars at the ages of 2, 7, 28 and 90 days are provided in Table 6. The mean values of the flexural strength of mortars without SS solution are decreased with the increase in WBP content for both binary cements with up to 40% WBP and ternary cements with 50% of WBP+GGBFS. There is a significant difference in flexural strength between C100 and all binary/ternary cements at all ages except for C90B10 at 2 days ($p = 0.51$). For ternary cements with 50% PC replacement without SS solution (C50B10S40, C50B25S25 and C50B40S10), using 10–40% GGBFS to replace the PC shows lower mean values than the corresponding binary cements with the same content of WBP (C90B10, C75B25 and C60B40) at 2 and 7 days, while the comparative results are insignificant at 28 and 90 days ($p > 0.05$). In addition, compared with C50S50, the flexural strength of C50B10S40 is insignificant at 2, 7, 28 and 90 days ($p > 0.05$), and that of C50B25S25 is insignificant at 2 and 7 days ($p > 0.05$), while C50B40S10 shows a significant difference at 7, 28 and 90 days. In comparison to mortars without SS, the addition of 1.5 and 2.5% SS obviously increases the flexural strength of the corresponding mixture at 2 days. Compared with C60B40 without SS, C60B40 with 1.5% SS shows a higher mean flexural strength at 7 days while the difference is insignificant at 28 and 90 days ($p > 0.05$). Furthermore, C60B40 with 2.5% SS shows an insignificant difference in flexural strength at 7 and 28 days ($p > 0.05$); however, the difference is significant at 90 days and the mean value is lower in comparison with C60B40 without SS. In the presence of GGBFS, the flexural strengths of C50B25S25 and C50B40S10 activated by SS solution show a significant difference with the corresponding ternary cements without SS at all ages ($p < 0.05$) and the mean value is higher, while the difference between C50B10S40 with and without 1.5% SS is insignificant ($p > 0.05$). The C50B10S40 with 2.5% SS shows a lower value than that without SS at 28 days. Furthermore, ternary cements with 1.5 and 2.5% SS show an insignificant difference with C100 at 90 days ($p > 0.05$), except for C50B40S10 with 1.5% SS. In addition, with the increase in SS content from 1.5 to 2.5%, the flexural strength of C50B10S40 at 2, 7, 28 and 90 days is decreased while the values of C50B25S25 and C50B40S10 are increased at 28 and 90 days.

Table 6. Flexural strength of mortars (N/mm^2).

Mixture	2 Days		7 Days		28 Days		90 Days		
	Mean	Std	Mean	Std	Mean	Std	Mean	Std	
0% SS	C100	5.0	0.4	8.2	0.4	9.7	0.3	9.8	0.3
	C50S50	2.5	0.1	4.7	0.3	7.6	0.2	8.4	0.5
	C90B10	4.4	0.2	5.6	0.1	6.7	0.2	8.4	0.2
	C75B25	3.5	0.1	4.6	0.2	6.7	0.3	7.3	0.1
	C60B40	2.2	0.3	4.2	0.3	5.5	0.1	6.7	0.5
	C50B10S40	2.2	0.1	4.7	0.3	7.4	0.3	8.2	0.3
	C50B25S25	2.1	0.1	4.1	0.1	6.1	0.2	7.1	0.5
	C50B40S10	2.0	0.1	3.5	0.2	5.4	0.1	6.1	0.4
1.5% SS	C60B40	3.7	0.3	5.4	0.3	5.2	0.2	7.1	0.1
	C50B10S40	3.6	0.2	5.9	0.3	7.4	0.2	9.3	0.1
	C50B25S25	3.4	0.1	5.1	0.1	7.0	0.3	9.3	0.1
	C50B40S10	2.9	0.2	5.1	0.1	6.0	0.4	8.6	0.1
2.5% SS	C60B40	3.6	0.4	4.0	0.3	4.8	0.3	7.9	0.2
	C50B10S40	3.7	0.1	3.8	0.1	5.4	0.2	9.1	0.2
	C50B25S25	3.4	0.2	6.0	0.2	8.4	0.6	10.6	0.1
	C50B40S10	3.0	0.2	4.8	0.1	6.6	0.1	9.5	0.1

Table 7 shows the compressive strength results of mortars at the ages of 2, 7, 28 and 90 days. There is a significant difference between C100 and all other mortars with/without SS ($p < 0.05$) at all ages and C100 shows the highest value. C50S50 and C50B10S40 exhibit approximately 3% and 13% lower values than C100 at 90 days, respectively, due to a high content of GGBFS with latent hydraulic properties. In addition, the compressive strength of mortars without SS is decreased with the increase in WBP content for both binary cements with up to 40% WBP and ternary cements with 50% of WBP+GGBFS at 2, 7, 28 and 90 days. Compared with binary cements with the same WBP content (C90B10, C75B25 and C60B40), using 10–40% GGBFS to replace the PC (C50B10S40, C50B25S25 and C50B40S10) decreases the compressive strength at 2, 7 and 28 days while it increases the value at 90 days. Figure 5a shows the compressive strength ratio of binary cements over the C100. The compressive strength of C90B10, C75B25 and C60B40 is lower than 90%, 75% and 60% of the compressive strength of C100, respectively at all ages. Figure 5b shows the compressive strength ratio of blended cements with 50% of WBP+GGBFS over C100. The compressive strength ratio is lower than 0.5 at 2 days for all blended cements with 50% of WBP+GGBFS. Moreover, the compressive ratio is increased with the increase in GGBFS content, and the higher the GGBFS content, the earlier the compressive strength ratio exceeds the value of 0.5. At 90 days, the compressive strength ratio for all blended cements with 50% of WBP+GGBFS is higher than 0.5. Hence, the WBP with low pozzolanic activity (Table 5) seems to contribute mainly to the dilution effect on the development of compressive strength, while the contribution of GGBFS is obvious from 7 days (C100 vs. C50S50).

Table 7. Compressive strength of mortars (N/mm²).

Mixture	2 Days		7 Days		28 Days		90 Days		
	Mean	Std	Mean	Std	Mean	Std	Mean	Std	
0% SS	C100	25.2	1.2	45.5	0.8	56.4	2.1	66.1	0.8
	C50S50	9.8	0.2	24.7	1.5	47.1	1.5	62.1	2.7
	C90B10	19.7	0.1	28.7	1.3	37.5	0.6	51.6	1.5
	C75B25	13.6	0.2	23.0	1.5	36.8	1.2	36.9	2.0
	C60B40	7.5	0.3	18.1	0.7	27.4	0.6	34.3	0.9
	C50B10S40	8.4	0.2	22.3	0.4	40.8	0.9	57.5	1.2
	C50B25S25	7.2	0.1	19.8	0.7	33.2	1.1	44.4	1.4
	C50B40S10	7.4	0.1	15.1	0.8	25.3	1.1	35.0	0.7
1.5% SS	C60B40	13.4	0.5	17.8	0.9	25.0	0.4	26.6	0.7
	C50B10S40	11.6	0.6	21.3	0.6	36.5	0.9	38.3	0.9
	C50B25S25	12.2	0.1	20.7	0.6	31.6	0.8	36.3	0.2
	C50B40S10	11.5	0.4	19.1	2.3	20.9	1.5	29.1	0.2
2.5% SS	C60B40	12.5	0.8	15.7	0.6	20.5	0.7	30.4	0.7
	C50B10S40	11.8	0.6	15.5	0.3	21.0	0.8	42.2	1.7
	C50B25S25	10.8	0.5	20.5	1.3	29.4	1.4	43.1	0.4
	C50B40S10	9.3	0.4	15.5	0.7	22.4	1.3	33.5	0.4

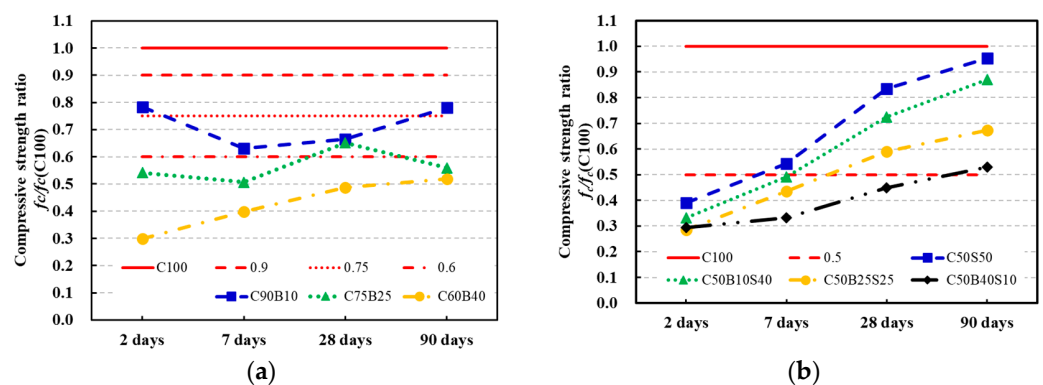


Figure 5. The compressive strength ratio of blended cements without SS over C100 based on mean values at 2, 7, 28 and 90 days: (a) binary cements with 10–40% WBP; (b) binary and ternary cements with 50% of WBP+GGBFS.

In the case of SS addition, there is a significant difference in the compressive strength of C60B40 between 0%, 1.5% and 2.5% SS ($p < 0.05$), and the compressive strength of mortars with 1.5% and 2.5% SS is higher than those without SS at 2 days. At 7 days, C60B40 without SS shows an insignificant difference in compressive strength to C60B40 with 1.5% and 2.5% SS ($p > 0.05$). At 28 days, there is an insignificant difference between C60B40 and C60B40 with 1.5% SS ($p = 0.16$), while the difference between C60B40 and C60B40 with 2.5% SS is significant ($p < 0.05$) and C60B40 shows a higher value. At 90 days, C60B40 shows a significant difference in compressive strength to C60B40 with 1.5% and 2.5% SS ($p < 0.05$), and C60B40 shows a higher value. When adding the SS solution in blended cement, the SS reacts with $\text{Ca}(\text{OH})_2$ from PC hydration to form NaOH and CaSO_4 . In the literature, it is mentioned that, when using 1–6% Na_2O equivalent of SS (for comparison: 0.65% and 1.3% Na_2O equivalent of SS in this paper) to activate pure GGBFS, the pH value in the pore solution ranges from 12.0 to 12.3, which is lower than the approximate pH value of 13 from PC hydration [24,27]. As aforementioned, the WBP in blended cement with 10–40% WBP mainly contributes to the dilution effect as seen from the compressive strength results. Hence, because of the lower pH value related to the reaction of SS, it is probably difficult to activate the WBP with a pozzolanic activity as low as that used in this study, and the presence of CaSO_4 may dominate the effect on the performance of blended cement with 40% WBP or 50% of WBP+GGBFS. In [33], the quick dissolution of aluminates and ferrite in the PC hydration process creates an oversaturated pore solution of aluminium ions, which retards the hydration rate of silicates as the surface of silicates is poisoned by the absorption of aluminate ions. The presence of CaSO_4 can react rapidly with the aluminates to produce ettringite, resulting in a decrease in aluminium concentration in the pore solution and an increase in silicate hydration [34,35]. In [36], the hydration of tricalcium silicate (C_3S) in PC is accelerated with the increase in CaSO_4 content from 0 to 6% (related to the mass of C_3S) at 1 and 2 days since the adsorption of CaSO_4 on the C–S–H surface modifies the nucleation-growth process, leading to a higher compressive strength at early ages. Hence, the rapid consumption of aluminium ions in pore solution due to the addition of 1.5% and 2.5% SS promotes ettringite generation and silicate hydration, leading to a higher compressive strength at 2 days. In addition, the reduction in the compressive strength of blended cements with 1.5% and 2.5% SS at 28 and 90 days is possibly attributed to the reduction in PC hydration with the addition of SS. In [37], although the mechanism remains unclear, the degree of white PC hydration is decreased in the presence of 4.1% SS (mass related to PC mass), which increases the total/capillary porosity of mortars and reduces the compressive strength at 7, 28 and 90 days. More research is required to elucidate the reaction mechanisms and phase assemblages of PC in the presence of SS.

In the presence of GGBFS, there is a significant difference in compressive strength at 2 days between mortars with and without SS solution for ternary cements with 50% of WBP+GGBFS ($p < 0.05$), and the compressive strength of ternary cements with 1.5% or 2.5% SS is higher than that without SS at 2 days. The CaSO_4 accelerates PC hydration and reduces the total and capillary porosity at 2 days, as mentioned above in [37]. Moreover, the addition of CaSO_4 to ternary cements can reduce the aluminium ion content in pore solution, which promotes GGBFS hydration and prevents the destabilization of ettringite to mono-sulphates, resulting in a high early strength at 2 days [25]. Compared with the strength of mortars without SS at 7 days, C50B40S10 activated by 1.5% SS solution shows a significant difference ($p < 0.05$) and a lower mean value, while the difference is insignificant when adding 2.5% SS solution ($p > 0.05$). Furthermore, the compressive strength of C50B25S25 shows insignificant differences between the addition of 0, 1.5 and 2.5% SS at 7 days. For C50B10S40 with a high GGBFS content, the difference in compressive strength is insignificant between mortars with 1.5% SS and without SS ($p = 0.93$) at 7 days, while mortars with 2.5% SS show a significant difference with mortars without SS ($p < 0.05$). The mortars with 2.5% SS show a higher mean compressive strength than mortars with 0% and 1.5% SS at 7 days. Compared with corresponding mixtures without SS at 28 and 90 days, mortars with 1.5 and 2.5% SS show a significant difference in compressive strength

($p < 0.05$) and the mean value is lower, except for C50B25S25 with 1.5% SS at 28 days ($p = 0.40$), C50B25S25 with 2.5% SS at 90 days ($p = 0.43$) and C50B40S10 with 2.5% SS at 90 days ($p = 0.24$). In addition, mortars with 1.5% SS show a higher strength value at 7 and 28 days, while the mean value is lower at 90 days compared with mortars with 2.5% SS. From [27,37–40], the mechanism by which the addition of SS in blended cement with GGBFS reduces the late strength after 7 days remains unclear but may be related to the effects of CaSO_4 . On the one hand, the addition of CaSO_4 can increase the ettringite content with GGBFS hydration over time, which contributes to a positive effect on the late compressive strength [40]. On the other hand, the $[\text{SO}_4]^{2-}$ in CaSO_4 can react with the aluminium in C-A-S-H gel produced from GGBFS hydration to form ettringite, which destabilizes the C-A-S-H structure [37–39]. Moreover, in [41,42], different hydration products exhibit different strength contributions, in which C-S-H dominates for the development of strength. Hence, the reduction in compressive strength at late ages is probably due to the decrease in C-A-S-H content, while the increase in ettringite content may alleviate this reduction to some extent. However, further research is needed to elucidate these effects.

3.4. Carbonation

The carbonation results of mortars at 14, 42 and 68 days are shown in Figure 6. The results show that the carbonation depth is increased with the increase in WBP content for both binary cements with 10–40% WBP and ternary cements with 50% of WBP+GGBFS. C90B10 exhibits an insignificant difference in carbonation depth to C100 at 14, 42 and 68 days ($p > 0.05$), while the other mortars with/without SS show higher carbonation depths than C100 due a lower $\text{Ca}(\text{OH})_2$ content. Compared with their corresponding mixture without SS, C60B40 and C50B40S10 with 1.5 and 2.5% SS show a significant difference in carbonation depth at all ages ($p < 0.05$) and the mean values are lower. There is a significant difference in carbonation depth at 14 and 42 days between C50B25S25 with and without SS solution ($p < 0.05$) and mortars with 1.5 and 2.5% SS show lower values, while the difference is insignificant at 68 days ($p > 0.05$). The positive effect of SS solution on the carbonation depth is observed for blended cements with a low GGBFS content (C60B40 and C50B40S10) at 14, 42 and 68 days. However, the C50B10S40 mixtures with 1.5 and 2.5% SS show an insignificant difference in carbonation depth to that without SS at 14 days ($p > 0.05$), while the difference is significant at 42 and 68 days ($p < 0.05$). The carbonation depths of C50B10S40 with 1.5 and 2.5% SS are higher than that without SS at 42 and 68 days. The carbonation resistance of mortars depends on a trade-off between the positive and negative effects of 1.5% and 2.5% SS. The positive effects of SS on carbonation resistance are possibly due to pore refinement in these mixes or pore blockage during carbonation. In [40], the pore volume of large pores (diameter > 200 nm) in mortars with 100% GGBFS activated by 5.0% SS (mass related to GGBFS mass) is reduced. Hence, pore refinement via an increase in ettringite volume with the addition of SS solution can reduce CO_2 permeability. Moreover, [43] showed that for pastes with 100% GGBFS activated by NaOH at 1% CO_2 concentration, the reaction between Na^+ , OH^- , CO_2 and H_2O in the pore solution forms NaHCO_3 , $\text{Na}_2\text{CO}_3 \cdot \text{NaHCO}_3 \cdot 2\text{H}_2\text{O}$ and $\text{NaCa}(\text{CO}_3)_2 \cdot 5\text{H}_2\text{O}$, which can contribute positively to pore blockage and a reduction in CO_2 ingress. In contrast, the possible drying shrinkage of mortars with 1.5% and 2.5% SS shows negative effects on the carbonation resistance. From [44], the drying shrinkage of 100% GGBFS activated by 1% SS (mass related to powder mass) is obviously higher than that of 95% GGBFS + 5% PC at 20 ± 1 °C and $60 \pm 10\%$ RH. Although none of the aforementioned references correspond exactly with our case, they give some indication of the possible reasons behind the enhanced performances of the mixes with the SS activator. Future work in this area is required to determine the details of the mechanisms taking place in the case of mixtures with WBP (and GGBFS).

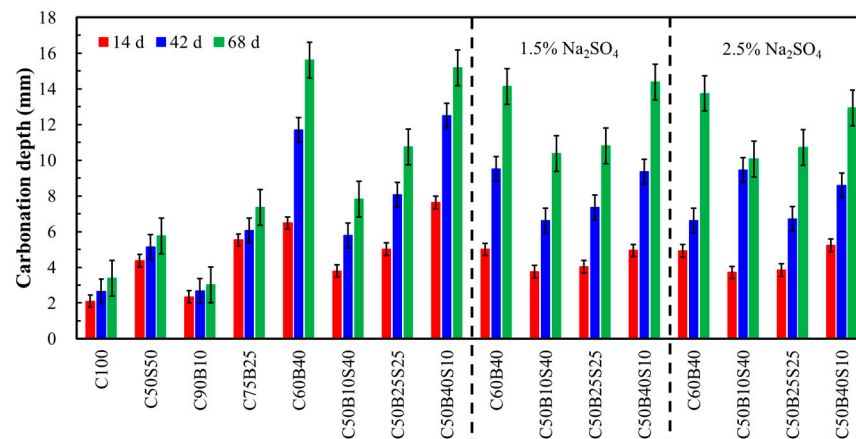


Figure 6. The carbonation depth of mortars at 14, 42 and 68 days of storage in the carbonation chamber ($T = 20 \pm 2$ °C, $RH = 60 \pm 10\%$ and 1% CO_2 level).

3.5. Non-Steady-State Chloride Migration

Figure 7 shows the values of the non-steady-state chloride migration coefficients of the mortars after 28-day and 56-day storage in a water tank. The results indicate that the chloride migration coefficient of mortars without SS is increased with the increase in WBP content in both binary cements with 10–40% WBP and ternary cements with 50% of WBP+GGBFS since the poor pozzolanic activity of the WBP leads to a reduction in hydration products and increases the porosity. For ternary cements with 40% GGBFS+quartz, the pore entry size is increased with the increase in quartz content from 10% to 40%, as reported in [45]. C90B10 shows a slightly higher migration coefficient than C100 at 28 and 56 days. Moreover, the blended cements with high GGBFS content (C50S50, C50B10S40 and C50B25S25) show a lower chloride migration coefficient than C100, probably due to the pore refinement from GGBFS hydration. As was mentioned in [45–47], binary cements with 40% or 50% GGBFS show a lower pore size distribution and average pore diameter at 28 days compared with PC. For mortars with 1.5 and 2.5% SS solution, the chloride migration coefficient is significantly different from the corresponding mortars without SS ($p < 0.05$), and mortars with 1.5 and 2.5% SS show obviously lower values. In [37,40], for mixes with 100% GGBFS activated by 5.0% SS (mass related to GGBFS mass), the pore structure is refined and the critical pore radius is decreased in the presence of SS at 28 days, resulting in a low chloride migration coefficient.

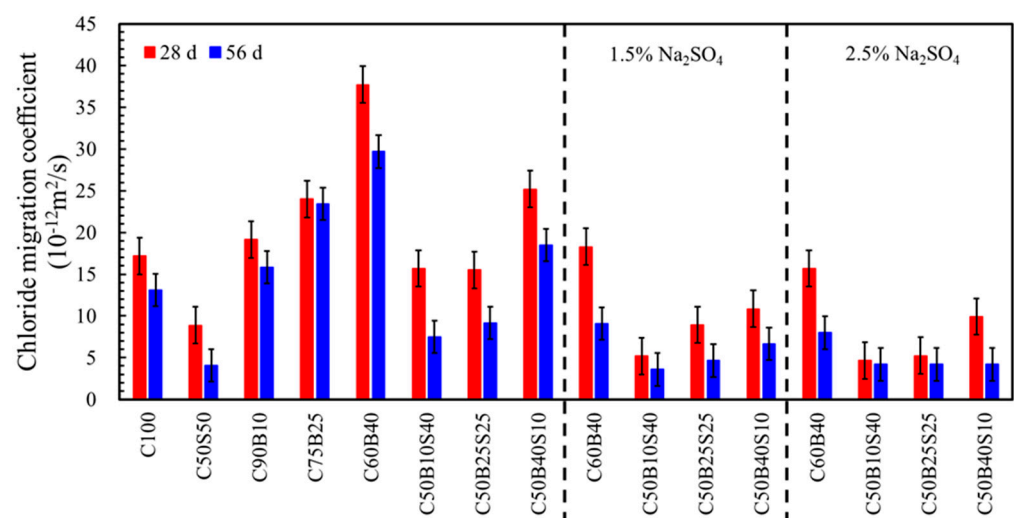


Figure 7. Chloride migration coefficient of mortars after 28 and 56 days of curing in a water tank at 20 °C.

4. Conclusions

The main conclusions are as follows:

1. The amorphous content and Frattini test indicate that the WBP used in this study has low pozzolanic activity.
2. The fresh and hardened properties of both binary and ternary cements are decreased with the increase in WBP content from 10% to 40% since the WBP with low pozzolanic activity mainly contributes to the dilution effect. Compared with C100, C90B10 exhibits a similar carbonation depth after 14, 42 and 68 days of exposure and a slightly higher chloride migration coefficient at the age of 28 and 56 days.
3. For ternary cements with 50% PC replaced by WBP+GGBFS, the flexural and compressive strengths are increased while the carbonation depth and chloride migration coefficient are decreased with the increase in GGBFS content. Compared with C100, C50S50 and C50B10S40 exhibit approximately 3% and 13% lower compressive strengths at 90 days and an obviously lower chloride migration coefficient at 28 and 56 days.
4. The addition of 1.5 and 2.5% SS solution increases the compressive strength of binary cement with 40% WBP and ternary cement with 10–40% WBP and 40–10% GGBFS at 2 days, while the compressive strength at 28 and 90 days is decreased since the presence of SS probably destabilizes the C-(A)-S-H structure. The carbonation depth of mortars at 14, 42 and 68 days is decreased with the addition of 1.5 and 2.5% SS solution. However, the C50B10S40 with 1.5 and 2.5% SS exhibits a higher carbonation depth at 42 and 68 days than that without SS. In addition, mortars with 1.5 and 2.5% SS show a lower chloride migration coefficient at 28 and 56 days than mortars without SS.

Author Contributions: Conceptualization, E.G.; Methodology, Z.Z., S.P. and E.G.; Formal analysis, Z.Z. and S.P.; Investigation, Z.Z. and S.P.; Writing—original draft, Z.Z. and S.P.; Writing—review & editing, E.G.; Supervision, E.G.; Funding acquisition, E.G. All authors have read and agreed to the published version of the manuscript.

Funding: This research was funded by [CHINA SCHOLARSHIP COUNCIL] grant number [201906370008].

Data Availability Statement: Data are contained within the article.

Conflicts of Interest: The authors declare no conflict of interest.

References

1. NBN EN 197-1; Cement-Composition, Specifications and Conformity Criteria for Common Cements. NBN (Bureau for Standardisation): Brussel, Belgium, 2011; pp. 1–41.
2. EN 197-5:2021; Cement-Part 5: Portland-Composite Cement CEM II/C-M and Composite Cement CEM VI Cement. European Committee for Standardisation: London, UK, 2021; Volume 1, pp. 2–5.
3. Karen, L.S.; John, V.M.; Gartner, E.M. Eco-Efficient Cements: Potential, Economically Viable Solutions for a Low-CO₂, Cement-Based Materials Industry. *World Bus. Counc. Sustain. Dev.* **2016**, *42*, 8–21. Available online: <https://spiral.imperial.ac.uk/bitstream/10044/1/51016/2/2016-UNEP%20Report-Complete6.pdf> (accessed on 23 October 2023).
4. Fatta, D.; Papadopoulos, A.; Avramikos, E.; Sgourou, E.; Moustakas, K.; Kourmoussis, F.; Mentzias, A.; Loizidou, M. Generation and Management of Construction and Demolition Waste in Greece—An Existing Challenge. *Resour. Conserv. Recycl.* **2003**, *40*, 81–91. [\[CrossRef\]](#)
5. Reig, L.; Tashima, M.M.; Borrachero, M.V.; Monzó, J.; Cheeseman, C.R.; Payá, J. Properties and Microstructure of Alkali-Activated Red Clay Brick Waste. *Constr. Build. Mater.* **2013**, *43*, 98–106. [\[CrossRef\]](#)
6. Shao, J.; Gao, J.; Zhao, Y.; Chen, X. Study on the Pozzolanic Reaction of Clay Brick Powder in Blended Cement Pastes. *Constr. Build. Mater.* **2019**, *213*, 209–215. [\[CrossRef\]](#)
7. Navrátilová, E.; Rovnaníková, P. Pozzolanic Properties of Brick Powders and Their Effect on the Properties of Modified Lime Mortars. *Constr. Build. Mater.* **2016**, *120*, 530–539. [\[CrossRef\]](#)
8. Pacheco-Torgal, F.; Jalali, S. Reusing Ceramic Wastes in Concrete. *Constr. Build. Mater.* **2010**, *24*, 832–838. [\[CrossRef\]](#)
9. Katzer, J. Strength Performance Comparison of Mortars Made with Waste Fine Aggregate and Ceramic Fume. *Constr. Build. Mater.* **2013**, *47*, 1–6. [\[CrossRef\]](#)
10. Schackow, A.; Stringari, D.; Senff, L.; Correia, S.L.; Segadães, A.M. Influence of Fired Clay Brick Waste Additions on the Durability of Mortars. *Cem. Concr. Compos.* **2015**, *62*, 82–89. [\[CrossRef\]](#)

11. Li, H.; Dong, L.; Jiang, Z.; Yang, X.; Yang, Z. Study on Utilization of Red Brick Waste Powder in the Production of Cement-Based Red Decorative Plaster for Walls. *J. Clean. Prod.* **2016**, *133*, 1017–1026. [[CrossRef](#)]
12. Ortega, J.M.; Letelier, V.; Solas, C.; Moriconi, G.; Climent, M.Á.; Sánchez, I. Long-Term Effects of Waste Brick Powder Addition in the Microstructure and Service Properties of Mortars. *Constr. Build. Mater.* **2018**, *182*, 691–702. [[CrossRef](#)]
13. Rakhimova, N.R.; Rakhimov, R.Z. Alkali-Activated Cements and Mortars Based on Blast Furnace Slag and Red Clay Brick Waste. *Mater. Des.* **2015**, *85*, 324–331. [[CrossRef](#)]
14. Fořt, J.; Vejmelková, E.; Koňáková, D.; Alblová, N.; Čáchová, M.; Keppert, M.; Rovnaníková, P.; Černý, R. Application of Waste Brick Powder in Alkali Activated Aluminosilicates: Functional and Environmental Aspects. *J. Clean. Prod.* **2018**, *194*, 714–725. [[CrossRef](#)]
15. Zhao, Y.; Gao, J.; Liu, C.; Chen, X.; Xu, Z. The Particle-Size Effect of Waste Clay Brick Powder on Its Pozzolanic Activity and Properties of Blended Cement. *J. Clean. Prod.* **2020**, *242*, 118521. [[CrossRef](#)]
16. Bilim, C.; Ati, C.D. Alkali Activation of Mortars Containing Different Replacement Levels of Ground Granulated Blast Furnace Slag. *Constr. Build. Mater.* **2012**, *28*, 708–712. [[CrossRef](#)]
17. Angulo-Ramírez, D.E.; Mejía de Gutiérrez, R.; Puertas, F. Alkali-Activated Portland Blast-Furnace Slag Cement: Mechanical Properties and Hydration. *Constr. Build. Mater.* **2017**, *140*, 119–128. [[CrossRef](#)]
18. Kaja, A.M.; Lazaro, A.; Yu, Q.L. Effects of Portland Cement on Activation Mechanism of Class F Fly Ash Geopolymer Cured under Ambient Conditions. *Constr. Build. Mater.* **2018**, *189*, 1113–1123. [[CrossRef](#)]
19. Farasat, S.; Shah, A.; Chen, B.; Yousefi, S.; Haque, M.A.; Riaz, M. Improvement of Early Strength of Fly Ash-Slag Based One-Part Alkali Activated Mortar. *Constr. Build. Mater.* **2020**, *246*, 118533. [[CrossRef](#)]
20. Reig, L.; Tashima, M.M.; Soriano, L.; Borrachero, M.V.; Monzó, J.; Payá, J. Alkaline Activation of Ceramic Waste Materials. *Waste Biomass Valoriz.* **2013**, *4*, 729–736. [[CrossRef](#)]
21. Robayo, R.A.; Mulford, A.; Munera, J.; Mejía de Gutiérrez, R. Alternative Cements Based on Alkali-Activated Red Clay Brick Waste. *Constr. Build. Mater.* **2016**, *128*, 163–169. [[CrossRef](#)]
22. Komnitsas, K.; Zaharaki, D.; Vlachou, A.; Bartzas, G.; Galetakis, M. Effect of Synthesis Parameters on the Quality of Construction and Demolition Wastes (CDW) Geopolymers. *Adv. Powder Technol.* **2015**, *26*, 368–376. [[CrossRef](#)]
23. Luukkonen, T.; Abdollahnejad, Z.; Yliniemi, J.; Kinnunen, P.; Illikainen, M. Cement and Concrete Research One-Part Alkali-Activated Materials: A Review. *Cem. Concr. Res.* **2018**, *103*, 21–34. [[CrossRef](#)]
24. Rashad, A.M.; Bai, Y.; Basheer, P.A.M.; Milestone, N.B.; Collier, N.C. Hydration and Properties of Sodium Sulfate Activated Slag. *Cem. Concr. Compos.* **2013**, *37*, 20–29. [[CrossRef](#)]
25. Xue, L.; Zhang, Z.; Wang, H. Hydration Mechanisms and Durability of Hybrid Alkaline Cements (HACs): A Review. *Constr. Build. Mater. Manuscr.* **2021**, *266*, 121039. [[CrossRef](#)]
26. Fernández-Jiménez, A.; Garcia-Lodeiro, I.; Maltseva, O.; Palomo, A. Hydration Mechanisms of Hybrid Cements as a Function of the Way of Addition of Chemicals. *J. Am. Ceram. Soc.* **2019**, *102*, 427–436. [[CrossRef](#)]
27. Zhang, J.; Tan, H.; Bao, M.; Liu, X.; Luo, Z.; Wang, P. Low Carbon Cementitious Materials: Sodium Sulfate Activated Ultra-Fine Slag/Fly Ash Blends at Ambient Temperature. *J. Clean. Prod.* **2021**, *280*, 124363. [[CrossRef](#)]
28. NBN EN 196-1; Method of Testing Cement-Part 1: Determination of Strength. NBN (Bureau for Standardisation): Brussels, Belgium, 2005; pp. 1–35.
29. NBN EN 196-5; Methods of Testing Cement-Part 5: Pozzolanicity Test for Pozzolanic Cement. NBN (Bureau for Standardisation): Brussels, Belgium, 2005; pp. 1–15.
30. NBN EN 1015-3; Methods of Test for Mortar for Masonry—Part 3: Determination of Consistence of Fresh Mortar by Flow Table. NBN (Bureau for Standardisation): Brussels, Belgium, 1999; pp. 1–12.
31. NBN EN 13295:2004; Products and Systems for the Protection and Repair of Concrete Structures-Test Methods-Determination of Resistance to Carbonation. NBN (Bureau for Standardisation): Brussels, Belgium, 2004; pp. 1–15.
32. NT Build 492 Concrete, Mortar and Cement-Based Repair Materials: Chloride Migration Coefficient from Non-Steady-State Migration Experiments. *Measurement* **1999**, 1–8. Available online: <https://www.nordtest.info/wp/1999/11/21/concrete-mortar-and-cement-based-repair-materials-chloride-migration-coefficient-from-non-steady-state-migration-experiments-nt-build-492/> (accessed on 23 October 2023).
33. Pustovgar, E.; Mishra, R.K.; Palacios, M.; d’Espinose de Lacaillerie, J.B.; Matschei, T.; Andreev, A.S.; Heinz, H.; Verel, R.; Flatt, R.J. Influence of Aluminates on the Hydration Kinetics of Tricalcium Silicate. *Cem. Concr. Res.* **2017**, *100*, 245–262. [[CrossRef](#)]
34. Joseph, S.; Skibsted, J.; Cizer, Ö. A Quantitative Study of the C3A Hydration. *Cem. Concr. Res.* **2019**, *115*, 145–159. [[CrossRef](#)]
35. Scrivener, K.; Ouzia, A.; Juilland, P.; Kunhi Mohamed, A. Advances in Understanding Cement Hydration Mechanisms. *Cem. Concr. Res.* **2019**, *124*, 105823. [[CrossRef](#)]
36. Bentur, A. Effect of Gypsum on the Hydration and Strength of C₃S Pastes. *J. Am. Ceram. Soc.* **1976**, *59*, 210–213. [[CrossRef](#)]
37. Mota, B.; Matschei, T.; Scrivener, K. Impact of NaOH and Na₂SO₄ on the Kinetics and Microstructural Development of White Cement Hydration. *Cem. Concr. Res.* **2018**, *108*, 172–185. [[CrossRef](#)]
38. Mota, B.; Matschei, T.; Scrivener, K. Impact of Sodium Gluconate on White Cement-Slag Systems with Na₂SO₄. *Cem. Concr. Res.* **2019**, *122*, 59–71. [[CrossRef](#)]

39. Fu, J.; Jones, A.M.; Bligh, M.W.; Holt, C.; Keyte, L.M.; Moghaddam, F.; Foster, S.J.; Waite, T.D. Mechanisms of Enhancement in Early Hydration by Sodium Sulfate in a Slag-Cement Blend—Insights from Pore Solution Chemistry. *Cem. Concr. Res.* **2020**, *135*, 106110. [[CrossRef](#)]
40. Tan, H.; Deng, X.; He, X.; Zhang, J.; Zhang, X.; Su, Y.; Yang, J. Compressive Strength and Hydration Process of Wet-Grinded Granulated Blast-Furnace Slag Activated by Sodium Sulfate and Sodium Carbonate. *Cem. Concr. Compos.* **2019**, *97*, 387–398. [[CrossRef](#)]
41. Termkhajornkit, P.; Vu, Q.H.; Barbarulo, R.; Daronnat, S.; Chanvillard, G. Dependence of Compressive Strength on Phase Assemblage in Cement Pastes: Beyond Gel-Space Ratio-Experimental Evidence and Micromechanical Modeling. *Cem. Concr. Res.* **2014**, *56*, 1–11. [[CrossRef](#)]
42. Zajac, M.; Rossberg, A.; Le Saout, G.; Lothenbach, B. Influence of Limestone and Anhydrite on the Hydration of Portland Cements. *Cem. Concr. Compos.* **2014**, *46*, 99–108. [[CrossRef](#)]
43. Bernal, S.A.; Provis, J.L.; Brice, D.G.; Kilcullen, A.; Duxson, P.; Van Deventer, J.S.J. Accelerated Carbonation Testing of Alkali-Activated Binders Significantly Underestimates Service Life: The Role of Pore Solution Chemistry. *Cem. Concr. Res.* **2012**, *42*, 1317–1326. [[CrossRef](#)]
44. Rashad, A.M. Influence of Different Additives on the Properties of Sodium Sulfate Activated Slag. *Constr. Build. Mater.* **2015**, *79*, 379–389. [[CrossRef](#)]
45. Berodier, E.; Scrivener, K. Evolution of Pore Structure in Blended Systems. *Cem. Concr. Res.* **2015**, *73*, 25–35. [[CrossRef](#)]
46. Divsholi, B.S.; Lim, T.Y.D.; Teng, S. Durability Properties and Microstructure of Ground Granulated Blast Furnace Slag Cement Concrete. *Int. J. Concr. Struct. Mater.* **2014**, *8*, 157–164. [[CrossRef](#)]
47. Choi, Y.C.; Kim, J.; Choi, S. Mercury Intrusion Porosimetry Characterization of Micropore Structures of High-Strength Cement Pastes Incorporating High Volume Ground Granulated Blast-Furnace Slag. *Constr. Build. Mater.* **2017**, *137*, 96–103. [[CrossRef](#)]

Disclaimer/Publisher’s Note: The statements, opinions and data contained in all publications are solely those of the individual author(s) and contributor(s) and not of MDPI and/or the editor(s). MDPI and/or the editor(s) disclaim responsibility for any injury to people or property resulting from any ideas, methods, instructions or products referred to in the content.